International Journal of Refrigeration 143 (2022) 182–191

Contents lists available at ScienceDirect

International Journal of Refrigeration

journal homepage: www.elsevier.com/locate/ijrefrig

Inherent capacity modulation of a linear refrigeration compressor

Modulation de la puissance inhérente d'un compresseur frigorifique linéaire

Zhennan Zhu [a,b], Kun Liang [b,*], Hongyue Chen [c], Zhongwei Meng [a]

[a] School of Automotive and Transportation, Xihua University, Chengdu 610039, China
[b] Department of Engineering and Design, University of Sussex, Brighton BN1 9QT, United Kingdom
[c] School of Mechanical Engineering, Liaoning Technical University, Fuxin, 123000, China

ARTICLE INFO

Keywords:
Linear compressor
Inherent capacity modulation
Modelling
Cooling load
Part load
Compressor stroke

Mots clés:
Compresseur linéaire
Modulation de la puissance inhérente
Modélisation
Charge de refroidissement
Charge partielle
Course du compresseur

ABSTRACT

Conventional refrigeration compressors sized for peak cooling load actually operate at partial load mostly which could cause excessive on-off cycling loss. Linear compressor could overcome this challenge by varying the compressor stroke in response to transient cooling load. The present work establishes a numerical model for the capacity modulation of linear compressor using R134a through changing the input voltage to meet the cooling load. The numerical model contains a linear compressor model (including three sub-models describing the in-cylinder thermodynamic process, the piston mechanical dynamic process and the electrical part behaviour, respectively) and an input voltage modulation loop. Experimental data are collected for the validation of the numerical model. The results show that the capacity modulation, aiming to meet the cooling load within the error of 5%, can be achieved through varying the input voltage while fixing temperatures of heat exchangers. An increased voltage brings increased compressor stroke and mass flow rate in a linear trend with the heat exchanger temperature unchanged. Lower input voltage leads to higher motor efficiency due to lower copper loss. At a fixed condenser temperature and cooling load, the inherent capacity modulation can save energy with evaporator temperature increasing as the power consumption decreases. At condenser temperature of 50 °C, 40 °C and 30 °C, the CoP only changes by 1.5%, 0.9% and 2.7% when the cooling load changes from 100 W to 200 W. The inherent capacity modulation will allow the linear compressor to maintain a high annual efficiency for refrigeration.

1. Introduction

There is a need to improve the performance of a vapour refrigeration system (VCR) for the concern of energy saving and environmental protecting. The refrigerator is a considerable energy consumer amongst the household appliances (consumes 17% of whole residential electricity) and is challenged by the increasingly strict regulations (Li et al., 2019; Yabe et al., 2005). Compressor, as the heart of a vapour refrigeration system, consumes more than 80% of the required power of the whole system (Jomde et al., 2018). Linear compressor, which is regarded as an increasing research interest, requires no crank-shaft mechanism and is directly driven by a linear motor (Liang et al., 2014). Thanks to the absence of the crank-shaft mechanism, a linear compressor can be compact and allows oil-free operation, leading to a lower friction loss and a higher efficiency compared to a conventional rotary one.

Abundant studies have been conducted on performance of linear compressor and comparison between linear compressor and conventional one. Liang (2014) proposed a refrigeration test rig driven by a prototype moving magnet linear compressor and made a comparison with a conventional crank-drive compressor. It was found that the linear compressor can provide higher motor efficiency especially at lower motor output powers. And the maximum overall adiabatic efficiency of the linear compressor is approximately 15% higher than that of the crank-drive one. Koh et al. (2002) experimentally investigated the performance of a Stirling cryocooler using a linear compressor. The results showed that an increased charging pressure can bring a decreased stroke and an increased natural frequency. Also, the driving force of the linear compressor showed the minimum value at natural frequency. Jiang et al. (2020) studied the performance of a linear compressor using different clearance volumes (the zone from the top of the piston to the cylinder head) from 0.4 to 0.8 mm with R1234yf as refrigerant. It was

* Corresponding author.
E-mail addresses: kun.liang@sussex.ac.uk (K. Liang), chenhongyue@lntu.edu.cn (H. Chen).

https://doi.org/10.1016/j.ijrefrig.2022.06.032
Received 17 February 2022; Received in revised form 22 June 2022; Accepted 28 June 2022
Available online 30 June 2022

Nomenclature

Abbreviation

A_p	Area of piston (m^2)
C	Capacitance (F)
CD	Damping coefficient (N*s/m)
CL	Clearance (mm)
CoP	Coefficient of performance
e	Specific internal energy (J/kg)
D_p	Diameter of piston (mm)
E	Internal energy (J)
f	Frequency (Hz)
f_{res}	Resonant frequency (Hz)
F	Force (N)
h	Enthalpy (kJ/kg)
i	Current (A)
k_{gas}	Gas spring stiffness (N/m)
k_s	Mechanical stiffness (N/m)
L	Inductance (H)
L_p	Length of piston (mm)
M	Mass (kg)
P	Pressure (bar)
$\dot{Q}$	Heat transfer (W)
R	Resistance (Ω)
T	Temperature (K)
U	Voltage (V)
$\dot{W}$	Power (W)
X	Displacement (mm)
$\dot{X}$	Velocity (m/s)
$\overline{X}$	Acceleration (m/s^2)

Greeks

α	Motor constant (N/A)
μ	Viscosity (Pa·s)
ζ	Damping ratio

concluded that a decreased clearance volume can bring an increased cooling capacity as well as an increased volumetric efficiency due to the increases in mass flow rate. Additionally, minimizing clearance showed significant benefit at high pressure ratio.

Capacity modulation is necessary for a compressor as the working condition is various thus different cooling load. Compared to the on/off controlling, capacity modulation can achieve a continuous operation thus can avoid the energy loss during the motor start-up stage thus a higher efficiency. Moreover, unlike a conventional compressor, linear compressor modulates the cooling capacity by changing the piston stroke, avoiding the constrain of the rated speed. The inherent capacity modulation should keep fixed temperature of the heat exchangers to keep a fixed temperature of the refrigerated space.

To date, researchers have conducted many studies for achieving the capacity modulation function for different kinds of compressors. Tassou et al. (1983) conducted a comparison of the performance between capacity modulated and conventional on/off controlled heat pumps. The capacity modulation was achieved by changing the rotary speed. It was found that the capacity modulation system can give 10% higher energy utilisation efficiency over the conventional system. However, as mentioned above, the change in rotary speed can cause off-resonance operation, which can suppress the improvement in efficiency. Kim and Groll (2007) proposed an integrated method of capacity modulation for a domestic using bowtie compressor. The results showed that the mass flow rate can be controlled from 50% to 100% using an electronic control valve. Linear compressor, compared with a crank-driven one, can achieve simultaneous modulation in both compressor stroke and operating frequency. Lee et al. (2008) conducted a study on the compressor efficiency of a linear compressor under the capacity modulation effect. It was found that the motor efficiency at small cooling capacity is higher than that at high cooling capacity, indicating the benefit that capacity modulation can bring at partial load. Liang (2017) has also illustrated the promising potential of the capacity modulation function of linear compressor and it has already been a great research interest.

Numerical modelling can help in designing, optimization and controlling of a vapour compression refrigeration system. It is also a less costly and time-saving research method compared to an experimental study. More importantly, an accurate prediction of inherent capacity modulation must be based on a precise model of the vapour refrigeration system as an accuracy is strongly required in computing the relationship between the input (voltage) and the outputs (current, compressor stroke, mass flow rate, etc.).

There are increasing studies on numerical model of refrigeration and heat pump system. Hosoz et al. (2011) developed an adaptive neuro-fuzzy inference system model to study the performance of a vapour compression refrigeration system using R134a through the parameters such as compressor power, heat transferred, mass flow rate and CoP. Experiments were also conducted to validate the model. The results showed excellent agreement between modelled and experimental data with mean relative error locating in the range of 0.83~6.24%. Koury et al. (2001) proposed two numerical models of a variable speed refrigeration system to study the transient and steady state behaviour separately. The results showed that a higher degree of superheat and CoP can be achieved by increasing the throttling area or controlling the rotational speed. As the heart and the power source of a vapour refrigeration system, the quality of the compressor model can majorly decide the accuracy of prediction. Pollak et al. (1979) established a mathematical model of a single piston oscillating compressor explaining certain properties of the compressor. The predicted data agreed well with the measured ones. However, the in-cylinder processes of compression and expansion were assumed to be ideally isentropic, and the linear motor model was a RL equivalent circuit without a capacitor, which can result in a large phase difference between voltage and current thus a high power consumption.

Zhang et al. (2020) established a comprehensive numerical model of a linear compressor contains the in-cylinder thermodynamic model, the piston mechanical model and the linear motor model. The results showed that the predicted mass flow rate agreed well with measured ones and the volumetric efficiency decreased with pressure ratio. However, there is still a need to put more model validation through comparing the waveform of current, piston displacement and velocity. Dang et al. (2016b, 2016a) studied the dynamic and thermodynamic characteristics of a moving-coil linear compressor in the Stirling-type pulse tube cryocooler through establishing a numerical model. Experimental validations were also conducted. The phase angle between the piston position and the current, the input current and the input electric power from the model showed good agreement with the measured data. It was observed that the operating frequency had a significant influence on colling capacity, motor efficiency and Carnot efficiency. However, the waveform of the piston displacement and the cylinder pressure were assumed to be sinusoidal due to the lack of a detailed thermodynamic model, and there was no capacitance term in the linear motor model, either. Kim et al. (2009) proposed a numerical model for a linear compressor containing a piston dynamic sub-model and a linear motor sub-model with a capacitance term considered. However, there was no governing equation for the in-cylinder compression and expansion process thus the accuracy still has a room for improvement. Bradshaw

(2012) developed a detailed comprehensive simulation model for a linear compressor consisting of an in-cylinder process model (including valves sub-model, leakage sub-model and heat transfer sub-model et al.) and a piston dynamic model. However, the electric model for linear motor was not considered thus the shaft force was simply assumed to be sinusoidal. Based on the linear compressor model, some studies on the capacity modulation characteristics have been conducted. Li (2020) proposed a numerical model for a VCR system consisting of a thermodynamic part and a piston dynamic part. The model shows great agreement with measured data in piston displacement waveform and P-V loop. But due to the lack of the linear motor sub-model, the performance of the electrical part cannot be predicted precisely.

To date, there are also studies trying to achieve the capacity modulation for linear compressors using numerical approaches. Kim et al. (2011);Kim and Jeong (2013) proposed an inherent capacity modulation and investigated the performance characteristics of the capacity-modulated linear compressor for home refrigerators. The results showed that the capacity could be modulated from 55% to 90% over a condensing temperature range of 15–50 °C. When the cooling capacity was changing due to the change in current, the CoP was nearly identical because the energy dissipation by the current is almost identical. This study can prove that the inherent capacity modulation can help the concern of efficiency as well as energy saving. However, the linear compressor numerical model simply regarded the compression and expansion processes as ideally adiabatic and it strictly required a higher LC resonant frequency than the electrical supply frequency, which may lead to a limitation of the appliance. Bradshaw et al. proposed a method of capacity control through varying the clearance based on the numerical model for a linear compressor mentioned in Bradshaw (2012). It was observed that the isentropic efficiency decreased with the clearance while the CoP increased with cooling capacity. However, due to the lack of linear motor model, the driving force was regarded as sinusoidal.

This study proposed a capacity modulation model for a linear compressor using R134a, which can achieve the varying compressor stroke but fixed heat exchanger temperatures by only changing the input voltage to meet the required cooling load. Experimental validation has also been conducted. The effect of capacity modulation of the linear compressor is investigated through the varying of the parameters of the linear compressor characteristics during the capacity modulation process. This study can provide a theoretical support for the practical application of the inherent capacity modulation on the linear compressor.

2. Numerical model

2.1. Modelling for the inherent capacity modulation

The inherent capacity modulation mainly consists of a linear compressor model and a voltage modulation loop. The linear compressor model contains an in-cylinder thermodynamic sub-model, a piston mechanical dynamic sub-model and a linear motor model, computing the parameters such as piston displacement, current, mass flow rate, etc. through an input voltage. The voltage modulation loop is to increase or decrease the input voltage to match the corresponding output cooling capacity with the cooling load.

There are some assumptions in this model listed as below:

- The ambient temperature is equal to the cylinder wall temperature (20 °C).
- Body temperature is constant.
- The suction and discharge valves are rigid bodies with the leakage neglected.
- The refrigerant at condenser outlet is saturated liquid and that at evaporator outlet is saturated vapour.
- The pressure drop in the heat exchangers are neglected.

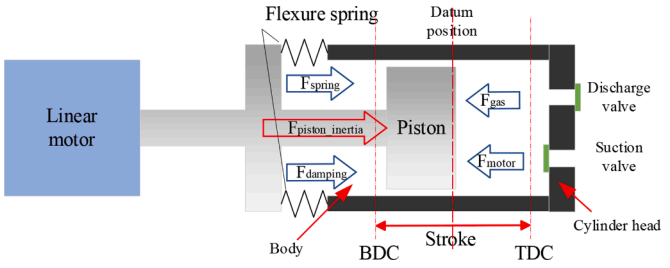

Fig 1. Schematic of linear compressor and forces acting on the piston (TDC: top dead centre, the position of the piston when it is at the top of its stroke; BDC: Bottom dead centre, when the piston is at the bottom of its stroke.) (Zhu et al., 2021).

- No enthalpy difference before and after the expansion valve.

2.1.1. Linear compressor model

The first part of the inherent capacity modulation model is the linear compressor model, which contains a thermodynamic sub-model, a mechanic dynamics sub-model and an electrical motor sub-model. The thermodynamic sub-model is applied in the compression chamber (the volume from the piston top face to the cylinder head) based on the mass and energy conservation equations, shown as below:

$$\frac{dE}{dt} = \dot{Q} + \dot{W} + \sum_{\text{in}} \dot{m}_{\text{in}} h_{\text{in}} - \sum_{\text{out}} \dot{m}_{\text{out}} h_{\text{out}} \tag{1}$$

$$\frac{dE}{dt} = \frac{d(e_c m_c)}{dt} = m_c \frac{de_c}{dt} + e_c \frac{dm_c}{dt} \tag{2}$$

where $\dot{Q}$ and $\dot{W}$ are the heat transfer and shaft work per time step. $\dot{m}_{\text{in}}$ and h_{in} denote the mass low rate and the enthalpy of the refrigerant into the compressor while $\dot{m}_{\text{out}}$ and h_{out} donate the mass low rate and the enthalpy of the refrigerant flowing out of the compressor. m_c is the refrigerant mass in the compressor cylinder and e_c denotes the specific internal energy, which can be expressed as below:

$$de = c_v dT + \left[T \left(\frac{\partial P}{\partial T} \right)_V - P \right] dV \tag{3}$$

$$e = h - PV \tag{4}$$

$$P = T \left(\frac{\partial P}{\partial T} \right)_V \tag{5}$$

where c_v, T, P and h represent the specific heat capacity at constant volume, temperature, pressure and specific enthalpy of the gas in cylinder, respectively.

The cylinder temperature change can be expressed through combining Eq. (1)–(5):

$$m_c c_v \frac{dT_c}{dt} + T_c \left(\frac{\partial P}{\partial T} \right)_V \left(\frac{dV_c}{dt} - \frac{1}{\rho} \frac{dm_c}{dt} \right) + h_c \frac{dm_c}{dt} = \dot{Q} + \sum_{\text{in}} \dot{m}_{\text{in}} h_{\text{in}} - \sum_{\text{out}} \dot{m}_{\text{out}} h_{\text{out}} \tag{6}$$

Then it can be transferred into:

$$\frac{dT_c}{dt} = \frac{1}{m_c c_v} \left[\dot{Q} + \sum_{\text{in}} \dot{m}_{\text{in}} h_{\text{in}} - \sum_{\text{out}} \dot{m}_{\text{out}} h_{\text{out}} - h_c \frac{dm_c}{dt} - T_c \left(\frac{\partial P}{\partial T} \right)_V \left(\frac{dV_c}{dt} - \frac{1}{\rho} \frac{dm_c}{dt} \right) \right] \tag{7}$$

The mass flowing out of the compressor ($\dot{m}_{\text{out}}$) will join the cycle of refrigeration thus is regarded as the mass flow rate. As the seal leakage needs to be considered, Liang (2014) proposed an equation, shown as Eq. (8):

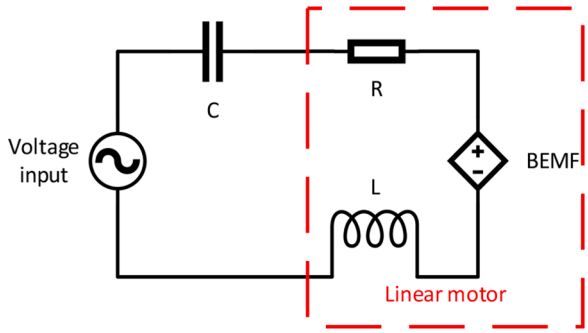

Fig 2. Equivalent electrical circuit of the linear compressor (Zhu et al., 2021).

$$\dot{m}_{\text{leak}} = \frac{\pi D_p C L^3 \left(P_c^2 - P_b^2\right)}{24 \mu L_p R_g T_c} \tag{8}$$

A linear compressor does not have a crank mechanism, instead the piston is directly driven by a linear motor, achieving the oscillating motion of the piston thus compression and expansion. A schematic of the linear compressor is shown as Fig.1. Two valves assembled on the cylinder head are aiming for suction and discharge and two flexure springs are aiming to force the piston back to the datum position. Four equivalent forces are functioning on the piston during the motion. The motor force (F_{motor}), which is the driving power source, is always in the same direction of piston motion while the damping force (F_{damping}) is opposite. The spring force (F_{spring}) is provided by the flexure springs thus towards the datum position. The gas force (F_{gas}), regarded as the pressure difference between the cylinder and the body timing the piston area, towards the body side. Finally, the inertia force ($F_{\text{piston\_inertia}}$) is the vector sum of all the forces mentioned.

Therefore, the mechanical dynamic sub-model of the piston can be written as below:

$$M_p \ddot{X}_p = \alpha i(t) + \left(P_c A_p - P_b A_p\right) - k_s X_p - C D_p \dot{X}_p \tag{9}$$

where $M_p \ddot{X}_p$ is the $F_{\text{piston\_inertia}}$ (M_p is the mass of the piston and $\ddot{X}_p$ is the acceleration of the piston, $\alpha i(t)$ denotes the F_{motor} (α is the motor constant through correlating (Liang, 2014) and $i(t)$ is the current), $(P_c A_p - P_b A_p)$ is the F_{gas} (P_c and P_b represent the cylinder and body pressure, A_p is the area of piston), $k_s X_p$ and $CD_p \dot{X}_p$ represent the F_{spring} and F_{damping}, respectively (k_s is the stiffness of the spring, CD_p is the damping coefficient, X_p and $\dot{X}_p$ represent the displacement and velocity of the piston).

The governing equation of the electric part of the linear compressor can be expressed as below:

$$U(t) = R i(t) + L \frac{di(t)}{dt} + \frac{1}{C} \int^{i} (t) dt + \alpha \dot{X}_p \tag{10}$$

where $U(t)$ is the input voltage, R, L and C denote the resistance, inductance and capacitance, respectively. $\alpha \dot{X}_p$ is the back electromotive force (BEMF) term. The equivalent circuit is shown in Fig.2.

2.1.2. Inherent capacity modulation

For a typical Brushless Direct Current (BLDC) reciprocating compressor, various operating frequency can help to obtain capacity modulation. However, the motor efficiency will fall when the compressor is operated off-design point. A linear compressor can achieve the capacity modulation through varying the compressor stroke by changing the input. This model is aiming to achieve the inherent capacity modulation with the temperature of the heat exchangers fixed. The detailed process of capacity modulation is described as below.

First of all, the mechanical input parameters and the electrical parameters should be given to the model as they will not change. The

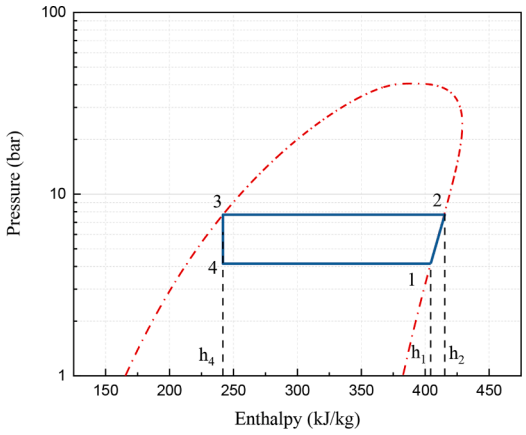

(a) *P-h* loop

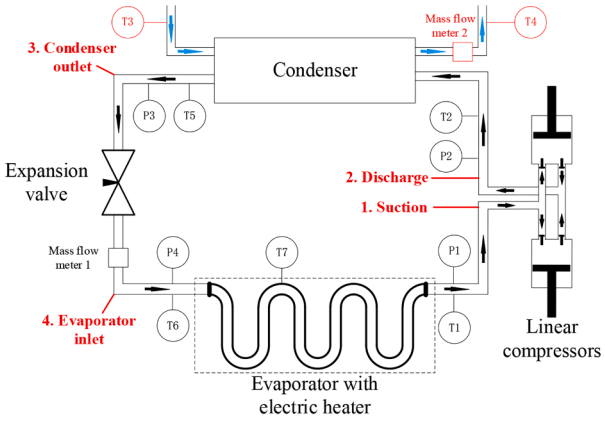

(b) Diagram of the test rig (T: thermometer; P: Pressure transducer)

Fig 3. P-h loop and diagram of the test rig of the linear compressor VCR system using R134a(a) P-h loop (b) Diagram of the test rig (T: thermometer; P: Pressure transducer).

mechanical input parameters include the mass of the piston M_p, the spring stiffness k_s, the damping coefficient CD_p and the piston area A_p. The electrical parameters include the resistance R, the inductance L, the capacitance C and the motor constant α. After that, a condenser temperature T_{cond} and an evaporator temperature T_{evap} will be set manually (can be different as working condition changes). Since the condenser temperature and evaporator temperature are set, the pressure ratio is also fixed. The body pressure P_b and body temperature T_b will also be given. The body pressure is 1~2 bar less than the mean in-cylinder pressure and the body temperature is set to be 40 °C according to the experimental data. The suction temperature T_s is set as 25 °C. According to the assumption for the model, the refrigerant at condenser outlet and evaporator outlet is regarded to be saturated. Thus, the thermodynamic properties of these point can be computed by calling the NIST REFPROP data base (Reference Fluid Thermodynamic and Transport Properties 2021) in the model.

Besides, a cooling load $\dot{Q}_{cd}$ should be set and a tolerance of ±10 W is set for the comparison between the actual cooling capacity and the cooling load, which means that if the difference between the computed cooling capacity and the cooling load is within the range of 10 W, then the cooling load is considered satisfied. To start the inherent capacity modulation model, an initial voltage input and a guess compressor stroke X_{pg} will be given for the calculation of the first step. In each step,

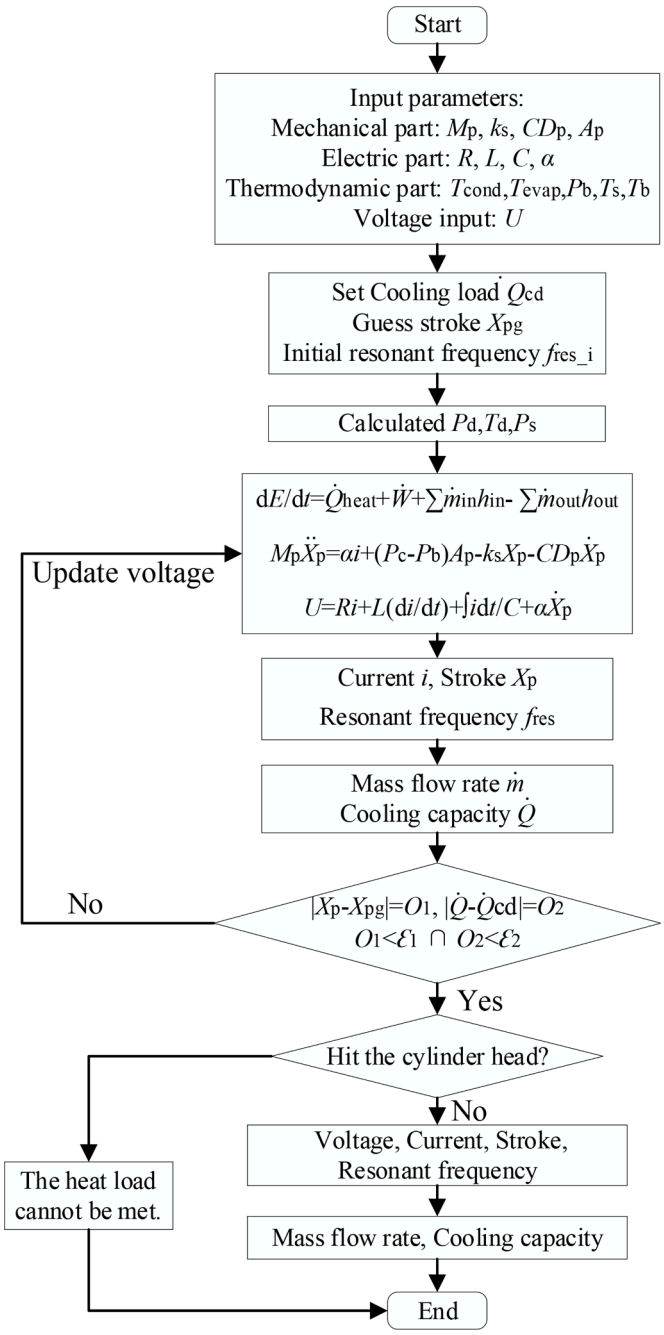

Fig 4. Flow chart of the inherent capacity modulation model.

an input voltage can lead to the calculation of the model and all the output parameters will be obtained such as the piston displacement, power consumption and cooling capacity, etc. After that, the obtained cooling capacity will be compared with the cooling load. If the difference is beyond the tolerance and the cooling capacity is lower than the cooling load, the voltage will increase by a step (set to be 0.8 V), otherwise the voltage will decrease by a step (set to be 0.4 V). This modulation will persist until the tolerance is satisfied. If the cooling load is too high, the calculated compressor stroke will beyond the limit (means hitting the cylinder head), thus the modulation will stop and return that the cooling load cannot be satisfied.

The increased compressor stroke means a larger swept volume by the piston. Since the suction and discharge pressures are fixed, a larger swept volume results in a higher mass flow rate $\dot{m}$ ($\dot{m}_{out}$ in Eq. (7)). A *P-h* loop of the vapour compression refrigeration system using R134a is

Fig 5. Photograph of the prototype linear compressor (Liang, 2014).

shown as Fig.3(a) with a diagram of the test rig shown as Fig.3(b). Since the refrigerant at condenser outlet is saturated liquid and that at evaporator outlet is saturated vapour, the dryness will be 0 and 1, respectively. Also, the pressure drop in the heat exchangers is neglected, so the pressures at condenser inlet and outlet are equal as well as the discharge pressure, same for the pressures at suction, evaporator inlet and outlet. The enthalpy at suction can be obtained through the pressure and the dryness at suction. The compression process is isentropic thus the entropy at suction and discharge are the same. The discharge temperature can be obtained through the pressure and entropy at discharge. Combining with the given temperatures and pressures of condenser, evaporator, suction and discharge, enthalpy at each point can be obtained using NIST REFPROP. The cooling capacity can be expressed using Eq. (11).

$$\dot{Q}_{cool} = \dot{m}\left(h_{evap\_out} - h_{evap\_in}\right) \tag{11}$$

The flowchart of the inherent capacity modulation is shown in Fig.4.

2.2. Model validation

A vapour refrigeration test rig using a prototype linear compressor is applied to conduct the experiments validating the model through the obtained voltage, piston displacement, mass flow rate and cooling capacity. The prototype linear compressor is shown as Fig.5. This test rig (shown as Fig.3(b)) has two prototype linear compressors (the schematic of piston-cylinder assembly is shown in Fig.1) in opposite direction for reducing the vibration. The condenser is an off-the-shelf water-cooled coaxial copper condenser, and the evaporator is an annular evaporator with an electric heater in it. The cooling load can be simulated by adjusting the power into the heater. The test rig mainly contains a main refrigeration cycle, a power and control part and a data acquisition part. The temperatures at compressor body, suction and temperature, condenser outlet, evaporator wall, inlet and outlet are measured by

Table 1
Key parameters of the linear compressor.

Parameters	Values
Capacitance (F)	0.00015
Damping Coefficient (N*s/m)	0.0475
Inductance (H)	0.141
Mechanical Stiffness (N/m)	16,284.85
Motor constant (N/A)	35
Moving mass (kg)	0.66
Piston area (mm^2)	283.23
Piston diameter (mm)	18.99
Piston length (mm)	31
Wire resistance (Ω)	3.5

Table 2
Test conditions of the linear compressor (simulation and measurement).

Refrigerant	R134a
Suction temperature (°C)	25
Condenser temperature (°C)	30,35,40,45,50
Evaporation temperature (°C)	8~20 (Experiment); −20~10 (Model)
Operating frequency (Hz)	37~39 (Experiment); 30~40 (Model)
Pressure ratio	2.5~3.5 (Experiment);1.5~10 (Model)
Cooling load (W)	20~500
Compressor stroke (mm)	< 15

seven K-type thermocouples (accuracy ±1.5 °C) (Thermocouple Selection Guide 2021). The pressures at compressor body, suction and discharge and evaporator inlet are measured by four Druck PMP1400 pressure transducers (accuracy ±0.15%). The currents of two compressors are measured by two LA LEM 25-NP current transducers (±0.5%) while the voltage is obtained by a Fylde 261 HVA HV voltage attenuator (±0.5%). An Electronic Wattmeter EW604 power metre is applied to get the real power of the electric heater in the evaporator (accuracy ±2.5%). The main mass flow rate and the bleed flow are measured by two thermal-type mass flow meters (Hastings HFM-201 and a Tylan FM-360 with accuracy of ±1%). The details of the test rig can be found in (Li, 2020). The key parameters of the linear compressor are displayed in Table 1 and the test conditions for the inherent capacity

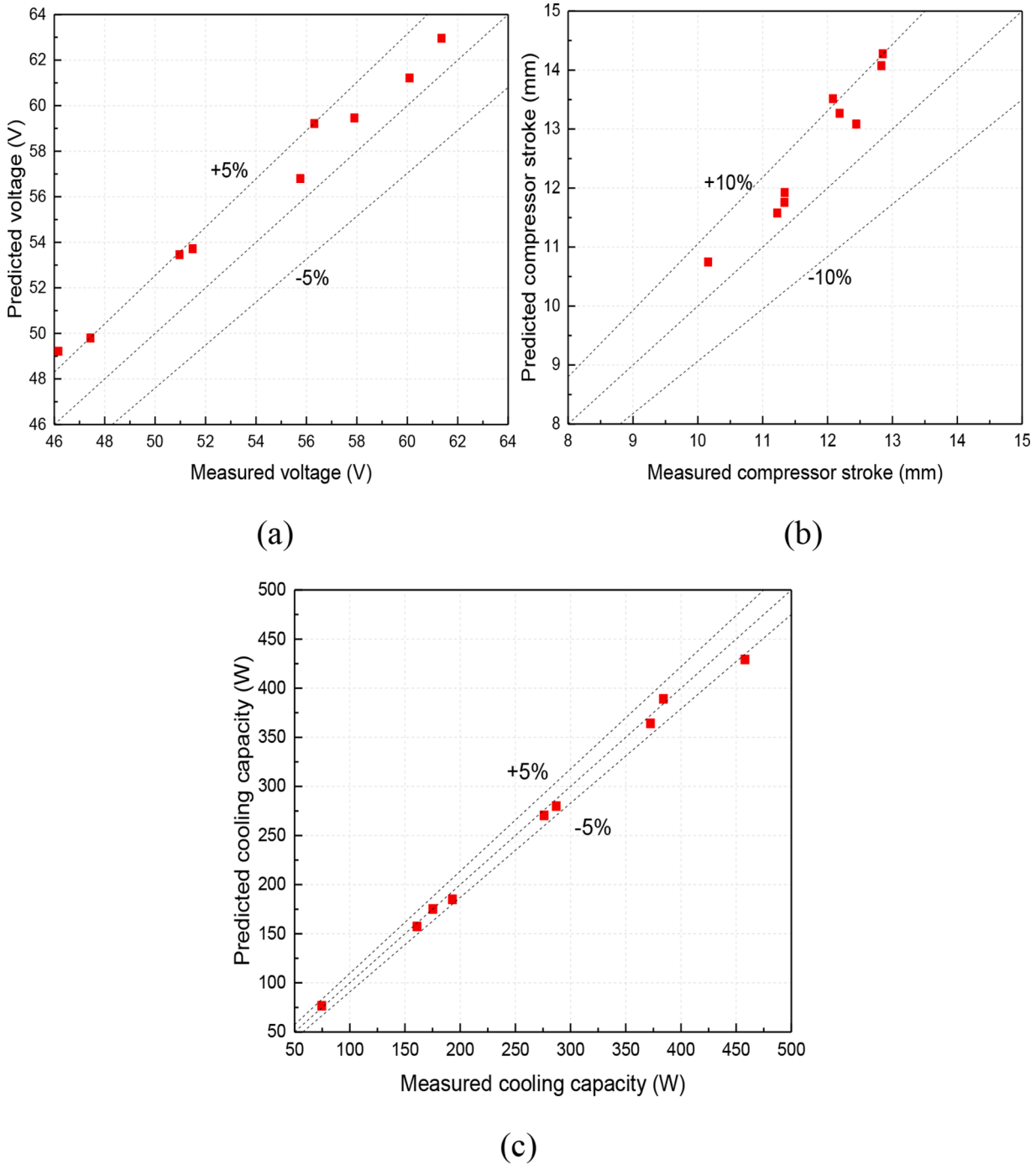

Fig 6. Model validation at the pressure ratio of 2.5, 3.0 and 3.5 and condenser temperature of 50 °C ((a) voltage; (b) compressor stroke; (c) cooling capacity).

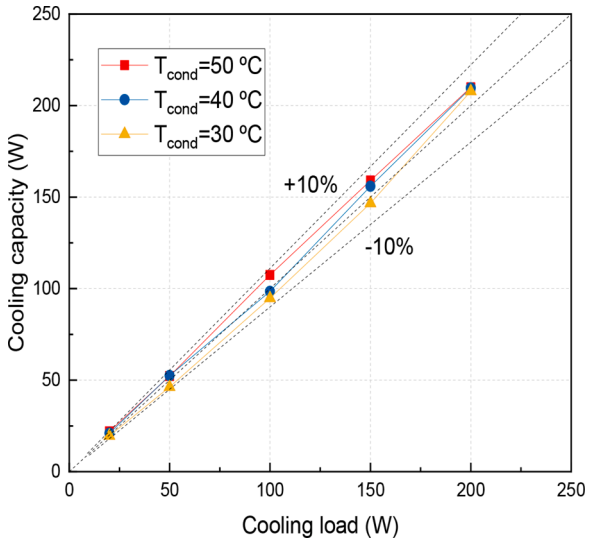

Fig 7. Cooling capacity against the cooling load at different condenser temperatures and evaporator temperature of 10 °C.

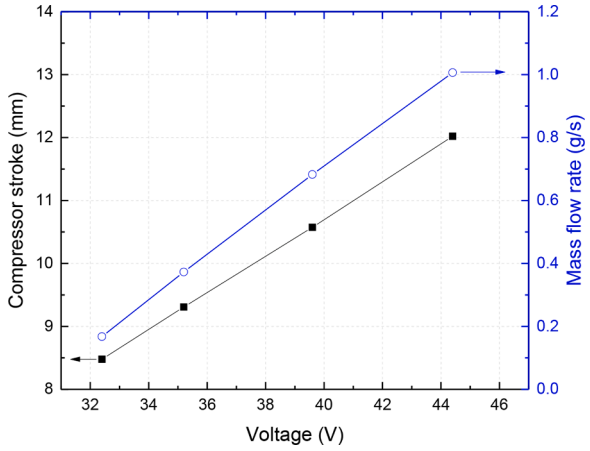

Fig 8. Compressor stroke and mass flow rate against the voltage at condenser temperature of 30 °C and evaporator temperature of 0 °C.

modulation model and experiments are listed in Table 2. It is needed to note that the conditions for the model and experiments are different as the experiments are only used to validate the model at lower pressure ratios but the model can provide the calculation for higher pressure ratios.

3. Results and discussion

Fig.6 plots the comparison between the measured voltage, compressor stroke and cooling capacity and the predicted ones from the model at the pressure ratio of 2.5, 3.0 and 3.5 and condenser temperature of 50 °C. It can be observed that the results from experiment and model agree well with most of the modelled voltage and cooling capacity dropping in an uncertainty within 5% and most of the modelled compressor stroke dropping in an uncertainty within 10%. The MAPE (mean absolute percentage error) can be calculated to have a better understand of the accuracy of the model, which is expressed as Eq. (12):

$$\mathrm{MAPE} = \frac{1}{n}\sum_{k=1}^{n}\left|\frac{EX_k - S_k}{EX_k}\right| \tag{12}$$

where EX_k and S_k represent the value from experiment and model, respectively. After calculation, the MAPEs of voltage, compressor stroke and cooling capacity are 3.9%, 7.2% and 1.7% respectively, indicating the high accuracy of the model.

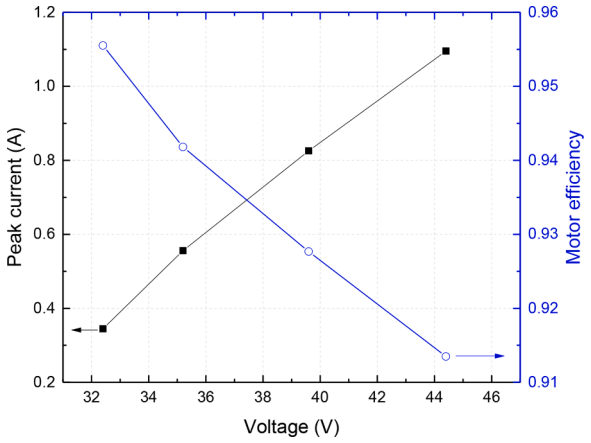

Fig 9. Peak current and motor efficiency against voltage at condenser temperature of 30 °C and evaporator temperature of 0 °C.

Fig.7 plots a comparison between the cooling capacity and the cooling load at condenser temperatures of 30 °C, 40 °C and 50 °C and evaporator temperature of 10 °C, confirming the availability and the accuracy of the inherent capacity modulation for the linear compressor. It is clear that the cooling capacity can increase with the cooling load and finally drop within the set tolerance (±10%). This is achieved by the corresponding automatic increase in voltage in the inherent capacity modulation model.

Fig.8 shows the compressor stroke and mass flow rate as functions of input voltage at condenser temperature of 30 °C and evaporator temperature of 0 °C. Note that a fixed condenser and evaporator temperature can lead to a fixed pressure ratio. The inherent capacity modulation can help to obtain different cooling capacity when the cooling load varies without changing the evaporator temperature, which can help to keep a constant temperature for the refrigerated space. It can be obtained from Fig.(8) that an increased voltage can bring an increased compressor stroke thus an increased mass flow rate. When the voltage increases from 32.4 V to 44.4 V, the compressor stroke can be modulated from 8.5 mm to 12.0 mm (41% increase) and the mass flow rate is modulated from 0.2 g/s to 1.0 g/s (400% increase), respectively. It can be observed that both compressor stroke and mass flow rate show a very linear trend with voltage (both with R-square beyond 0.999). However, the mass flow rate does not show a linear relationship with the piston stroke. Theoretically, volumetric flow rate can be calculated as Eq.(13).

$$\dot{V} = X * A * f \tag{13}$$

where X is the piston stroke, A is the crossing area and f is the operating frequency. It is seen that the volumetric flow rate is proportional to the stroke if the operating frequency is unchanged, and the mass flow rate is proportional to the stroke as well when the density is unchanged. However, in the actual process, which is also reflected in the model, the mass flow rate can be affected by the pressure drop across the reed valves, heat transfer during discharge and suction, leakage across the clearance. The linearity of mass flow rate against stroke also depends on the pressure ratio.

Fig.9 displays the peak current and motor efficiency as functions of input voltage at condenser temperature of 30 °C and evaporator temperature of 0 °C. It can be observed that an increased voltage can result in a larger current, thus higher cooling capacity requires higher power consumption. When the voltage increases from 32.4 V to 44.4 V, the peak current has increased by 0.8 A (217.8%) while the motor frequency has decreased by 4.2 Hz (4.4%). This is because the copper loss (i^2R) increases with the current. As the authors argued in previous research (Zhu et al., 2021), smaller compressor stroke requires lower voltage thus

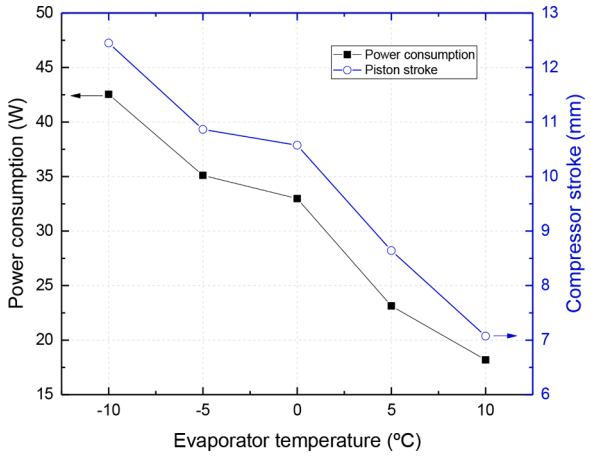

Fig 10. Power consumption and compressor stroke against evaporator temperature at condenser temperature of 30 °C and cooling load of 100 W.

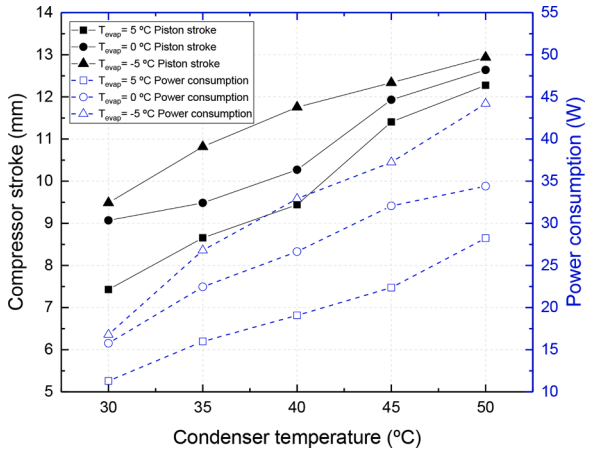

Fig 11. Compressor stroke and power consumption against condenser temperature at different evaporator temperatures and cooling load of 50 W.

lower power consumption and can cause lower CO_2 emission. As linear compressor mostly works at partial load, the linear compressor can show benefits of boosting the annual efficiency, thus can help to reach the achievement of being energy-saving and eco-friendly with the utilization of inherent capacity modulation.

Fig.10 plots the power consumption and compressor stroke against evaporator temperature at condenser temperature of 30 °C and different evaporator temperatures when the cooling load is 100 W. As the cooling load and condenser temperature are fixed, an increased evaporator temperature (can indicate a higher required temperature for the refrigerated space) means a lower pressure ratio. It can be seen that when the evaporator temperature rises, the compressor stroke and power consumption decrease. This is because that smaller pressure ratio can give larger mass flow rate at the same stroke. Therefore, when the cooling load is constant, lower evaporator temperature (higher pressure ratio) requires larger compressor stroke thus higher power consumption. When the evaporator increases from −15 °C to 10 °C, the power consumption has decreased by 24.4 W (133.9%) while the compressor stroke has decreased by 5.4 mm (76.0%). Nevertheless, it is observed that the decrease rate from evaporator temperature of −5 °C to 0 °C is reduced. The reason for this is that there may be errors in this model due to the assumptions such as the constant body pressure and temperature and these values may not be strictly accurate.

Fig.11 shows the compressor stroke and power consumption as functions of condenser temperature at different evaporator temperatures and cooling load of 50 W. When the evaporator temperature remains unchanged, higher condenser temperature means higher pressure ratio, which indicates that larger stroke is required for the same cooling load. It is clear that when the condenser temperature rises and the cooling load keeps unchanged, the compressor stroke increases thus the power consumption also rises. Also, lower evaporator temperature requires higher stroke at the same condenser temperature. It can be deduced that when the condenser temperature increases, the inherent capacity modulation can help to increase the power to satisfy the cooling demand. It can also help to decrease the power consumption as the pressure ratio decreases, thus can help for energy saving. When the condenser temperature rises from 30 °C to 50 °C, the compressor stroke rises by 4.8 mm (65.2%), 3.6 mm (39.3%) and 3.5 mm (36.3%) at evaporator temperature of −5 °C, 0 °C and 5 °C. It can be observed that at the high condenser temperature, the difference in compressor stroke is less significant but the power consumption shows significant difference amongst different evaporator temperatures. At the evaporator temperature of 0 °C and condenser temperature of 50 °C (close to a household fridge), the compressor stroke is 12.6 mm and the power consumption is 34.4 W when the cooling load is 50 W.

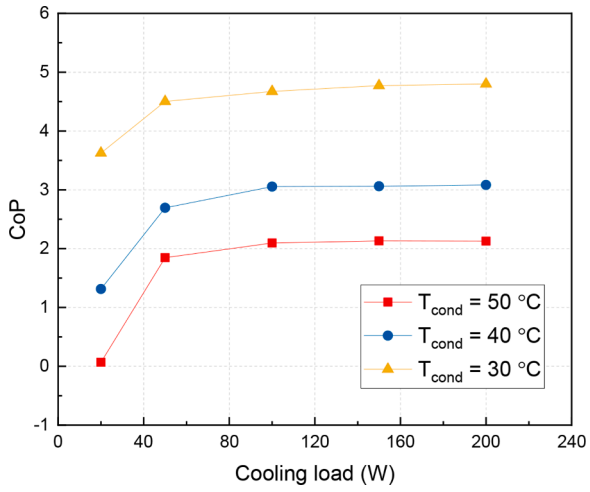

Fig 12. CoP as a function of cooling load at evaporator temperature of 10 °C.

Coefficient of performance (CoP) is an essential parameter of the performance of a VCR system reflecting the relation between the ability of cooling and consumption of power, written as Eq.(14).

$$\mathrm{CoP} = \frac{\dot{Q}_{\mathrm{cool}}}{\dot{W}} \tag{14}$$

where $\dot{Q}_{\mathrm{cool}}$ is the cooling capacity and $\dot{W}$is the power consumption, respectively.

Fig.12 plots the CoP as a function of cooling load when the evaporator temperature is 10 °C. It can be seen that CoP increases for the modulation process to a higher cooling load. The CoP is dramatically low at very low cooling load due to the very low cooling capacity. It can be seen that the CoP is much lower at a very low cooling capacity, which results from a low motor efficiency. It is also interesting to observe that the CoP varies very little when the cooling load is greater than 100 W. The differences in CoP when the cooling load changes from 100 W to 200 W are 1.5%, 0.9% and 2.7% for condenser temperature of 50 °C, 40 °C and 30 °C, respectively. This can indicate that the inherent capacity modulation can help the linear compressor to have the potential to reach a high annual performance as the linear compressor rarely works at the very low load or full load conditions. Meanwhile, when the evaporator temperature is fixed, the higher condenser temperature means a higher pressure ratio. Generally, a lower pressure ratio can bring a higher cooling capacity, thus a higher CoP, which also can be observed in Fig.12.

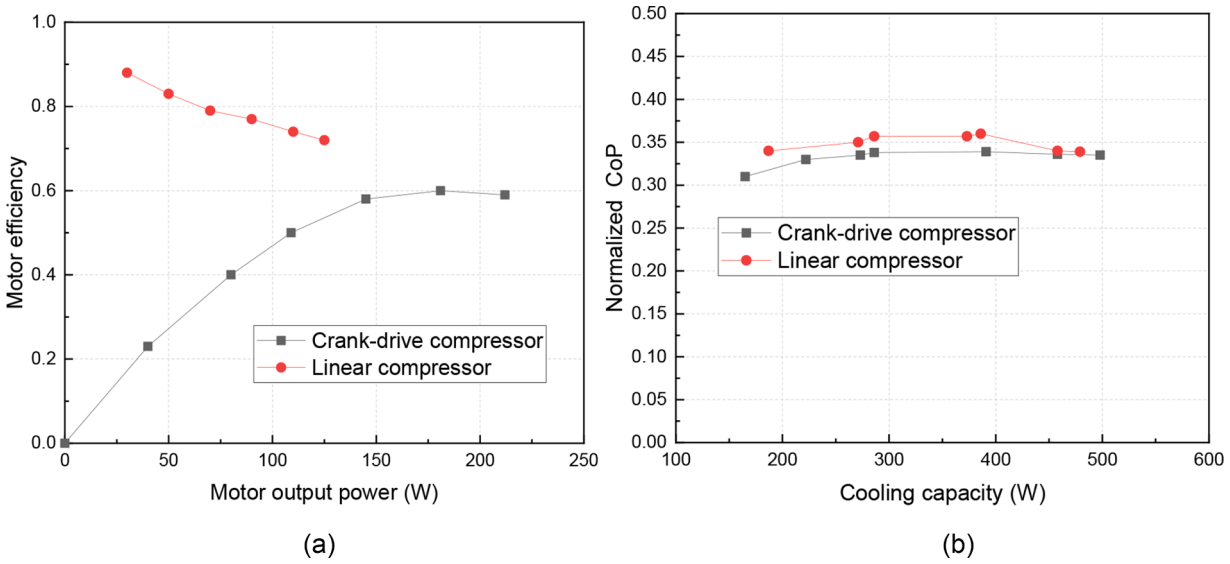

Fig 13. (a) Motor efficiency comparison between a linear compressor and a crank-drive compressor (Liang et al., 2014); (b) Normalized CoP comparison between a linear compressor and a crank-drive compressor (Liang et al., 2014).

It is meaningful to take an inverter-driven (crank-drive) compressors with similar scale for comparison to illustrate the advantages of linear compressors. Inverter-driven compressors modulate the cooling capacity through changing the rotation speed of the motor due to the fixed piston stroke constrained by the crankshaft mechanism. There are two problems associated with this method: (1) motor efficiency will drop from full load when the motor is operated off its rated speed; (2) a big current is needed to start the motor which will cause high copper loss (i^2R). Linear compressors, as illustrated in Fig.10, modulate the cooling capacity by changing the compressor stroke. There are two advantages associated with this method: (1) no big starting current is needed; (2) part load motor efficiency is even higher than full load because of lower copper loss.

Fig.13(a) shows the comparison of motor efficiency between the linear compressor and an inverter-driven compressor with similar scale. Lower cooling capacity will need a smaller current and high capacity needs a bigger current. This can show that the inherent capacity modulation has the potential benefit of automatic energy saving when the evaporator temperature (refrigerated space temperature) increases, i.e. the pressure ratio decreases.

Normalized CoP, which is the ratio of the steady-state CoP to the theoretically highest CoP, describes the thermodynamical perfectness of a refrigeration system and it makes more sense to use normalised CoP to compare two types of compressors. Fig.13(b) displays a comparison in normalized CoP between the prototype linear compressor and a crank-drive compressor. It can be seen that the linear compressor shows higher CoPs within the cooling capacity range.

4. Conclusion

This study illustrates an inherent capacity modulation model for a linear compressor. Experiments are conducted to compare with the modelled data for the validation. The performance characteristics such as compressor stroke, power consumption, resonant frequency and CoP of the linear compressor using R134a during the capacity modulation process are investigated at different condenser temperatures (30 °C, 40 °C and 50 °C) and evaporator temperatures (−20 °C~10 °C) as well as different cooling loads (20~200).Here are main conclusions.

1) The inherent capacity modulation model agrees well with experiments and can finally give a cooling capacity meeting the cooling load within a tolerance of ±10 W with keeping resonance and fixed temperature of heat exchangers.
2) The capacity modulation is achieved by changing the voltage. When the condenser and evaporator temperatures are fixed, higher cooling load requires increased input voltage, leading to increased compressor stroke and mass flow rate showing a linear trend with voltage. The motor efficiency increases in the modulation process to a lower cooling capacity, indicating the advantage of boosting the annual efficiency brought by inherent capacity modulation as the linear compressor mostly works at partial load.
3) When the cooling load is fixed, the inherent capacity modulation can help to save energy when condenser temperature decreases and evaporator temperature increases as smaller compressor stroke is required. When the condenser and evaporator temperatures are 50 °C and 0 °C with a cooling load of 50 W, a power consumption of 34.4 W is consumed, resulting in a compressor stroke of 12.6 mm.
4) CoP increases during the modulation process to a higher cooling load generally but slightly varies when the cooling load is greater than 100 W at evaporator temperature of 10 °C, indicating the advantage that the inherent capacity modulation may help the linear compressor to reach a high annual performance as the linear compressor rarely works at the very low load or full load conditions.
5) Following this study, there are potential future work such as tracking the resonant frequency when the linear compressor is operating at different conditions. As the gas spring caused by the pressure difference on both sides of the piston does not change linearly with the compressor stroke, this can be a challenge but an interesting project.

Declaration of Competing Interest

None

Acknowledgement

The first author would like to express his appreciation to the Joint Scholarship of the CSC and the University of Sussex for funding his PhD.

Reference

Bradshaw, C.R., 2012. A Miniature-Scale Linear Compressor for Electronics Cooling. Purdue University.

Dang, H., Zhang, L., Tan, J., 2016b. Dynamic and thermodynamic characteristics of the moving-coil linear compressor for the pulse-tube cryocooler. Part A: theoretical analyses and modelling. Int. J. Refrig. 69, 480–496.
Dang, H., Zhang, L., Tan, J., 2016a. Dynamic and thermodynamic characteristics of the moving-coil linear compressor for the pulse-tube cryocooler: part B - experimental verifcations. Int. J. Refrig. 69, 497–504.
Hosoz, M., Ertunc, H.M., Bulgurcu, H., 2011. An adaptive neuro-fuzzy inference system model for predicting the performance of a refrigeration system with a cooling tower. Expert Syst. Appl. 38 (11), 14148–14155.
Jiang, H., Li, Z., Liang, K., 2020. Performance of a linear refrigeration compressor with small clearance volume. Int. J. Refrig. 109, 105–113.
Jomde, A., Anderson, A., Bhojwani, V., Kedia, S., Jangale, N., Kolas, K., Khedkar, P., 2018. Modelling and measurement of a moving coil oil-free linear compressor performance for refrigeration application using R134a. Int. J. Refrig. 88, 182–194.
Kim, H., Roh, C., Kim, J., Shin, J., Hwang, Y., Lee, J., 2009. An experimental and numerical study on dynamic characteristic of linear compressor in refrigeration system. Int. J. Refrig. 32, 1536–1543.
Kim, J., Groll, E.A., 2007. Feasibility study of a bowtie compressor with novel capacity modulation. Int. J. Refrig. 30, 1427–1438.
Kim, J.K., Jeong, J.H., 2013. Performance characteristics of a capacity-modulated linear compressor for home refrigerators. Int. J. Refrig. 36, 776–785.
Kim, J.K., Roh, C.G., Kim, H., Jeong, J.H., 2011. An experimental and numerical study on an inherent capacity modulated linear compressor for home refrigerators. Int. J. Refrig. 34 (6), 1415–1423.
Koh, D.Y., Hong, Y.J., Park, S.J., Kim, H.B., Lee, K.S., 2002. A study on the linear compressor characteristics of the Stirling cryocooler. Cryogenics (Guildf) 42 (6–7), 427–432.
Koury, R.N.N., Machado, L., Ismail, K.A.R., 2001. Numerical simulation of a variable speed refrigeration system. Int. J. Refrig. 24, 192–200.
Lee, H., Ki, S., Jung, S., Rhee, W., 2008. The innovative green technology for refrigerators - development of innovative linear compressor. Int. Compressor Eng. Conf. 1867. Paper.
Z. Li, Measurements and modelling of a novel oil-free refrigeration system, Doctoral Thesis (PhD), University of Sussex, 2020.
Li, Z., Liang, K., Jiang, H., 2019. Experimental study of R1234yf as a drop-in replacement for R134a in an oil-free refrigeration system. Appl. Therm. Eng. 153, 646–654.
Liang, K., 2014. A Novel Linear Electromagnetic-Drive Oil-Free Refrigeration Compressor, Doctoral thesis (PhD). University of Oxford.
Liang, K., 2017. A review of linear compressors for refrigeration. Int. J. Refrig. 84, 253–273.
Liang, K., Stone, R., Hancock, W., Dadd, M., Bailey, P., 2014. Comparison between a crank-drive reciprocating compressor and a novel oil-free linear compressor. Int. J. Refrig. 45, 25–34.
Pollak, E., Soedel, W., Cohen, R., Friedlaender, F., 1979. On the resonance and operational behavior of an oscillating electrodynamic compressor. J. Sound Vib. 67, 121–133.
Reference Fluid Thermodynamic and Transport Properties Database (REFPROP). Available: https://www.nist.gov/srd/refprop. (Oct. 2021).
Tassou, S.A., Marquand, C.J., Wilson, D.R., 1983. Comparison of the performance of capacity controlled and conventional on/off controlled heat pumps. Appl. Energy 14 (4), 241–256.
Thermocouple Selection Guide. Available: https://docs.rsonline.com/96d5/0900766b815e5302. pdf (Oct. 2021).
Yabe, M., Sakanobe, K., Kawakubo, M., 2005. High efficient motor drive technology for refrigerator. In: Proceedings of the fourth international symposium on environmentally conscious design and inverse manufacturing. ECO Design, pp. 708–709. IEEE.
Zhang, X., Ziviani, D., Braun, J.E., Groll, E.A., 2020. Theoretical analysis of dynamic characteristics in linear compressors. Int. J. Refrig. 109, 114–127.
Zhu, Z., Liang, K., Li, Z., Jiang, H., Meng, Z., 2021b. A numerical model of a linear compressor for household refrigerator. Appl. Therm. Eng. 198, 117467.
Zhu, Z., Liang, K., Li, Z., Jiang, H., Meng, Z., 2021a. Thermal-economic-environmental analysis on household refrigerator using a variable displacement compressor and low-GWP refrigerants. Int. J. Refrig. 123, 189–197.

Further reading

Li, Z., Jiang, H., Chen, X., Liang, K., 2020. Optimal refrigerant charge and energy efficiency of an oil-free refrigeration system using R134a. Appl. Therm. Eng. 164, 114473.
Rao, S.S., 2004. Mechanical Vibrations. Prentice Hall fourth ed.